

Study on the Interaction of an Anthracycline Disaccharide with DNA by Spectroscopic Techniques and Molecular Modeling

Yan Lu · Gong-Ke Wang · Juan Lv · Gui-Sheng Zhang · Qing-Feng Liu

Received: 30 January 2010 / Accepted: 27 September 2010 / Published online: 16 October 2010
© Springer Science+Business Media, LLC 2010

Abstract This study was designed to examine the interaction of 4'-*O*-(α -L-Cladinosyl) daunorubicin (DNR-D5), a disaccharide anthracycline with calf thymus deoxyribonucleic acid (ctDNA) by UV/Vis in combination with fluorescence spectroscopy and molecular modeling techniques under physiological conditions (Britton–Robinson buffer solutions, pH=7.4). By the analysis of UV/Vis spectrum, it was observed that upon binding to ctDNA the anthraquinone chromophore of DNR-D5 could slide into the base pairs. Moreover, the large binding constant indicated DNR-D5 had a high affinity with ctDNA. At the same time, fluorescence spectra suggested that the quenching mechanism of the interaction of DNR-D5 to ctDNA was a static quenching type. The binding constants between DNR-D5 and ctDNA were calculated based on fluorescence quenching data at different temperatures. The negative ΔG implied that the binding process was spontaneous, and negative ΔH and negative ΔS suggested that hydrogen bonding force most likely played a major role in the binding of DNR-D5 to ctDNA. Moreover, the results obtained from molecular docking corroborate the experimental results obtained from spectroscopic investigations.

Keywords DNR-D5 · ctDNA · Fluorescence spectroscopy · UV/Vis · Molecular modeling

Introduction

The study on the interaction of small molecules with DNA is very important in many areas [1–4]. It is significant not only in understanding the mechanism of interaction, but also for guiding the design of new drugs. Based on these reasons, it is necessary to understand the modes and the factors that affected the binding of small molecules to DNA [5–8]. So more and more attentions have been paid to this area [9–14].

Small molecules bind to DNA by two predominant binding modes, intercalation and minor groove-binding. Intercalators bind to DNA by insertion of a planar, aromatic substituent between base pairs, simultaneously lengthening and unwinding the helix. Intercalators vary in the extent to which they unwind DNA, but all lengthen DNA to about the same extent [15]. In minor groove-binding, the crescent-shaped ligand fits into the minor groove with little steric hindrance and with little perturbation of the DNA structure [16]. The anthracycline antibiotics are arguably the best characterized DNA intercalators.

The anthracycline antibiotics daunorubicin have been used clinically since the 1990s [17]. So far, daunorubicin are considered to be the most important agents in use in cancer chemotherapy [18–20]. However, drug resistance and cardiotoxicity of anthracyclines limit their clinical application [21–23]. Many researchers have investigated various methods to modify the structure of daunorubicin to generate more analogs to reduce the side effects and reverse multidrug resistance; however, these efforts only have limited success. Recently, Sun and co-workers reported a novel class of disaccharide analogues of daunorubicin against drug-resistant leukemia [24, 25]. In these disaccharide analogues the first (inner) sugar in the carbohydrate

Y. Lu (✉) · G.-K. Wang · J. Lv · G.-S. Zhang · Q.-F. Liu
School of Chemistry and Environmental Science, Henan Normal University,
46 Jian-she Road,
Mu Ye District, Xinxiang 453007, China
e-mail: yanlu2001@sohu.com

chain is a daunosamine and the second sugars that linked to the first sugar are a series of uncommon sugars. Of all these disaccharide anthracyclines, 4'-*O*-(α -L-Cladinosyl) daunorubicin (DNR–D5, Fig. 1) emerged as the most active compound, showing similar antitumor activity against leukemia cell line K562 cells and colon cancer cell line SW620 cells to the parent compound DNR [24], and at least 5-fold higher activity against drug-resistant cells (K562/Dox) than DNR [25]. The compound DNR–D5 is worthy of further evaluation as a new drug candidate.

In the present work, the interaction of DNR–D5 with ctDNA was investigated under physiological (pH=7.4) conditions. The binding constant and binding sites were obtained utilizing the fluorescence method in combination with UV/Vis spectra and molecular modeling techniques. The binding mechanism and binding mode were completely elucidated at the same time. These results should be helpful for understanding the interaction of DNR–D5 with ctDNA at the molecular level and be useful for the design of new drugs.

Experimental

Materials

ctDNA was obtained from Sigma–Aldrich Chemicals Company (USA) and used without further purification. It was dissolved in doubly distilled water at a final concentration of 2.00×10^{-4} mol L⁻¹ and stored at 0–4 °C. The concentration was determined by the absorption of ctDNA at 260 nm after establishing the absorbance ratio of A_{260}/A_{280} in the range of 1.8–1.9, and the molarity of ctDNA was calculated based on $\epsilon_{260}=6600$ L mol⁻¹ cm⁻¹. pH value (pH=7.4) of the media was controlled with Britton–Robinson (BR) buffer solutions, which was prepared by adding the appropriate amount of 0.2 mol L⁻¹ NaOH into H₃BO₃, H₃PO₄ and HAc. DNR–D5 was synthesized according to the known method as a red solid and its spectra data were identical with those reported in literature [24]. The 1.00×10^{-3} mol L⁻¹ stock solution of DNR–D5 was prepared and used in all of the experiments. All other

reagents were of analytical reagent grade. Doubly distilled water was used throughout.

Apparatus and Methods

The UV/Vis spectra were obtained by using a TU-1810 spectrophotometer (Puxi Analytic Instrument Ltd., Beijing, China) equipped with 1.0 cm quartz cells. Fluorescence measurements were made on a Cary Eclipse fluorescence spectrophotometer (Varian, America) equipped with a 150 W Xenon flash lamp. The measurement of pH was performed on a PHS-2C pH-meter (Shanghai DaPu Instruments Co., LTD, Shanghai, China). The spectra measurement was thermostatically controlled by a SHP DC-0515 thermostatic bath (Shanghai Hengping Instruments Co., LTD, Shanghai, China).

UV/Vis Spectra Measurements

UV/Vis spectra measurements were carried out at 25 °C in the range of 200–350 nm. During the spectra titration, a constant concentration of DNR–D5 (10 μ M) was titrated with increasing concentration of ctDNA in 1 cm path length matched quartz cells. The ctDNA solutions of corresponding concentrations were measured as reference solutions.

Fluorescence Spectra Measurements

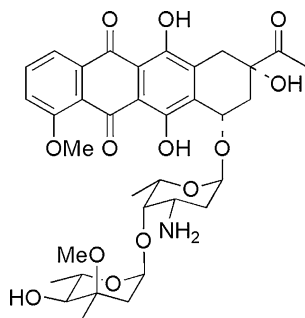
A 1.0 mL BR buffer solution (pH=7.4), a 100 μ L stock solution of DNR–D5 and vary volume of ctDNA solution were transferred to a 10 mL volumetric flask, and the mixed solution was diluted to the final volume with doubly distilled water. To evaluate the effect of temperature on DNA–DNR–D5 interaction, fluorescence was recorded at three different temperatures (290, 300 and 310 K). Throughout the fluorescence measurements, the excitation wavelength of DNR–D5 was 254.06 nm, the 5 nm \times 5 nm slit widths was used.

Results and Discussion

UV/vis Absorbance Spectroscopy Studies

Figure 2 shows the UV/Vis spectra of DNR–D5 in the absence and presence of ctDNA. In presence of increasing concentrations of ctDNA, the hypochromic effect is obviously observed. This hypochromic effect is thought to be due to the overlap of the π electron cloud of the anthraquinone chromophore of DNR–D5 with the ctDNA base pairs [26, 27]. Hypochromic effect in UV/Vis spectra upon ligand binding to DNA is a typical characteristic of an intercalating mode [28, 29]. These results indicate that the

Fig. 1 Structure of DNR–D5



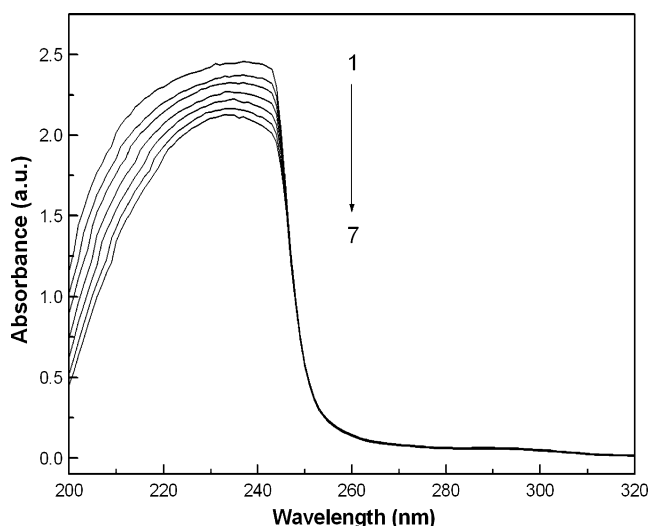


Fig. 2 UV/Vis spectra of the interaction between DNR–D5 and ctDNA in BR buffer solution (pH=7.4). $C_{\text{DNR-D5}}=10^{-5} \text{ mol L}^{-1}$, From 1 to 7: $C_{\text{DNA}}=0, 10^{-5}, 2 \times 10^{-5}, 3 \times 10^{-5}, 4 \times 10^{-5}, 5 \times 10^{-5}, 6 \times 10^{-5} \text{ mol L}^{-1}$

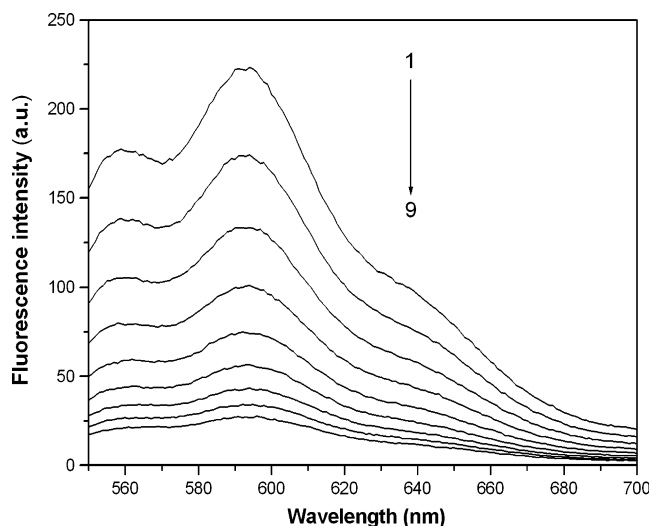


Fig. 4 Fluorescence emission spectra of the interaction between DNR–D5 and ctDNA in BR buffer solution (pH=7.4). The emission spectra of DNR–D5 were recorded with $\lambda_{\text{ex}}=254.06$, at 293 K. $C_{\text{DNR-D5}}=10^{-5} \text{ mol L}^{-1}$, From 1 to 9: $C_{\text{DNA}}=0, 10^{-5}, 2 \times 10^{-5}, 3 \times 10^{-5}, 4 \times 10^{-5}, 5 \times 10^{-5}, 6 \times 10^{-5}, 7 \times 10^{-5}, 8 \times 10^{-5} \text{ mol L}^{-1}$

anthraquinone chromophore of DNR–D5 can slide into the base pairs upon DNR–D5 binding to DNA, and the binding mode between DNR–D5 and ctDNA might be intercalation.

According to the variations in the absorbance spectra of drug upon binding to DNA, the binding constant (K), was calculated based on the equation [30]:

$$\frac{A_0}{A - A_0} = \frac{\varepsilon_G}{\varepsilon_{H-G} - \varepsilon_G} + \frac{\varepsilon_G}{\varepsilon_{H-G} - \varepsilon_G} \frac{1}{K[\text{DNA}]} \quad (1)$$

where A_0 and A are the absorbance of drug in the absence and presence of DNA, ε_G and ε_{H-G} are the absorption coefficients of drug and its complex with DNA, respectively. The plot of $A_0/(A-A_0)$ versus $1/[\text{DNA}]$ constructed using the data from the absorbance titrations is shown in Fig. 3.

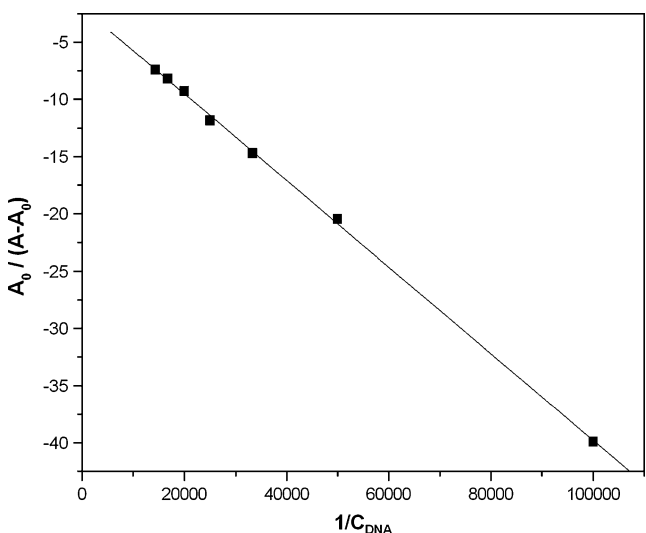


Fig. 3 The plot of $A_0/(A-A_0)$ versus $1/[\text{DNA}]$ at 25 °C

From the linear fitting, the binding constant (K) can be estimated from the ratio of the intercept to the slope. With this procedure, we calculated $K=5.220 \times 10^3 \text{ L mol}^{-1}$ ($R=0.9997$). It is seen that the fitting is good linear, and the value of K determined here is consistent with that reported for the DNA binding to anthracycline ($K \approx 10^3$ to 10^5 L mol^{-1}) [31]. This indicates that DNR–D5 display a relative high affinity with ctDNA.

Fluorescence Spectra

The binding of DNR–D5 to ctDNA was also examined by fluorescence titration measurement. An obvious decrease of the fluorescence of DNR–D5 was observed with increasing of ctDNA concentration (Fig. 4). This shows that DNR–D5 fluorescence is efficiently quenched upon binding to ctDNA. When the concentration of ctDNA was up to $8 \times 10^{-5} \text{ mol L}^{-1}$, the fluorescence intensity of DNR–D5 was almost completely quenched, indicating the binding reached saturation [32].

Table 1 The dynamic quenching constants between DNR-D5 and ctDNA at different temperatures

$T(\text{K})$	$K_{\text{SV}}(\text{L mol}^{-1})$	$k_q(\text{L mol}^{-1} \text{ s}^{-1})$	R^a
293	8.794×10^4	8.794×10^{12}	0.9893
303	6.815×10^4	6.815×10^{12}	0.9801
310	6.008×10^4	6.008×10^{12}	0.9869

R^a is the correlation coefficient

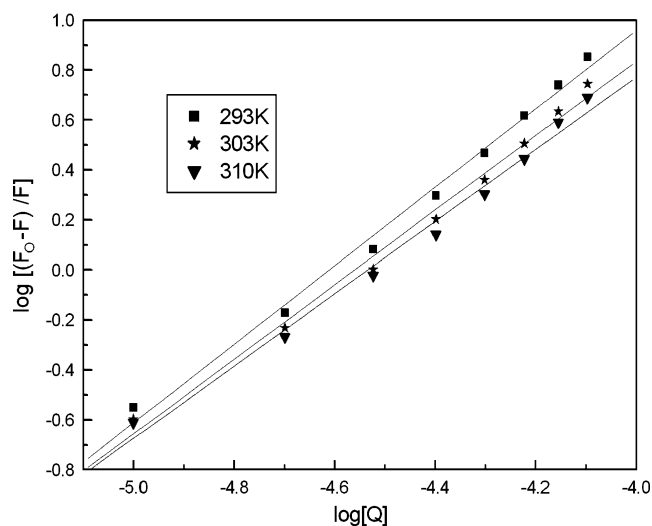


Fig. 5 The plot of $\log (F_0-F)/F$ versus $\log [Q]$ at different temperatures

Quenching Mechanism and Binding Constants

A quenching process can be usually induced by a collisional process which is dynamic quenching or a formation of a complex between quencher and fluorophore which is static quenching. Dynamic and static quenching can be distinguished by their differing dependence on temperature. Dynamic quenching depends upon diffusion. Since higher temperatures result in larger diffusion coefficients, the bimolecular quenching constants are expected to increase with increasing temperature. In contrast, an increase in temperature is likely to result in a decrease in stability of complexes, and thus lower values of the static quenching constants [33]. In order to confirm the quenching mechanism, the fluorescence quenching was analyzed according to the Stern-Volmer equation [34].

$$F_0/F = 1 + k_q \tau_0 [Q] = 1 + K_{SV} [Q] \quad (2)$$

where F_0 and F represent the steady-state fluorescence intensities in the absence and presence of quencher, respectively. $[Q]$ is the concentration of quencher. k_q is the quenching rate constant of bimolecule. τ_0 is the average lifetime of bimolecule without the quencher and its value is 10^{-8} s [35], and K_{SV} is the Stern-Volmer dynamic quenching constant, which was determined by linear regression of a

Table 2 The binding constants K_b and number of the binding sites n between DNR-D5 and ctDNA at different temperatures

$T(K)$	$K_b(L \text{ mol}^{-1})$	n	R^a
293	1.711×10^7	1.569	0.9962
303	6.263×10^6	1.491	0.9956
310	3.541×10^6	1.445	0.9943

R^a is the correlation coefficient

Table 3 The thermodynamic parameters for the DNR–D5 binding to ctDNA at different temperatures

$T(K)$	$\Delta G^0 (KJ \text{ mol}^{-1})$	$\Delta H^0 (KJ \text{ mol}^{-1})$	$\Delta S^0 (J \text{ mol}^{-1} \text{ K}^{-1})$
293	-40.54	-70.31	-101.63
303	-39.52	-70.31	-101.63
310	-38.88	-70.31	-101.63

plot of F_0/F against $[Q]$. According to Eq. 2, the quenching constant k_q was calculated to be about $10^{12} \text{ L mol}^{-1} \text{ s}^{-1}$ as listed in Table 1. However, the maximum scatter collision quenching constant k_q of various quenchers with the biopolymer is $2.0 \times 10^{10} \text{ L mol}^{-1} \text{ s}^{-1}$ [36], which suggests that the fluorescence quenching process may be mainly controlled by a static quenching mechanism rather than dynamic. From Table 1 we can also clearly see that K_{SV} is inversely correlated with temperature, which indicates again that the quenching is not caused by dynamic collision but comes from the formation of a complex. So fluorescence quenching mechanism of DNR–D5 by ctDNA is a static quenching type.

The binding constant K and the number of binding sites n of DNR–D5 with ctDNA are calculated by the following equation using the data from fluorescence titration:

$$\log(F_0 - F)/F = \log K_b + n \log [Q] \quad (3)$$

where in the present case, K_b is the binding constant and n is the number of the binding sites, which can be determined by the ordinate and slope of double logarithm regression curve (Fig. 5) of $\log (F_0-F)/F$ versus $\log [Q]$ based on the Eq. 3, respectively. The values of K_b and n are evaluated and presented in Table 2. From Table 2, it can be found that DNR–D5 may effectively bind to ctDNA with high affinity, and the ratio of binding of ctDNA to DNR–D5 is about

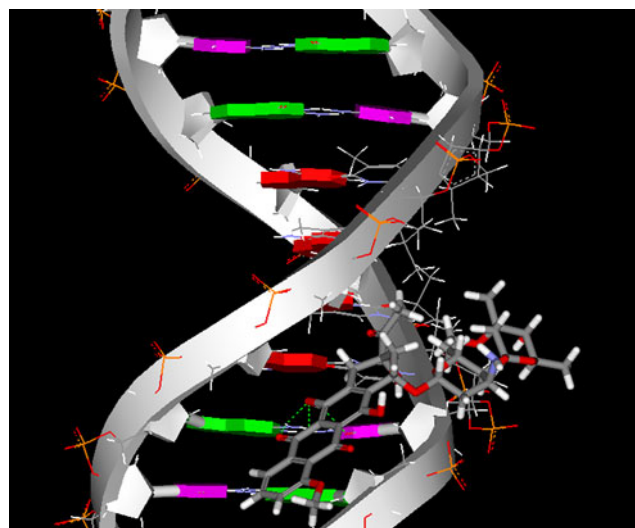


Fig. 6 Molecular modeling of DNR–D5 with ctDNA interaction

1:1.5. Additionally, we can also see that the values of K_b decrease with the increase in temperature, which is in good agreement with the trend of K_{sv} as mentioned above. It implies that an unstable complex may be formed in the binding reaction and the complex would possibly be dissociated partly when the temperature increases.

Binding Mode

The acting forces between a small molecular substance and DNA mainly include hydrogen bond, van der Waals force, electrostatic force, hydrophobic interaction force and so on. The signs and magnitudes of thermodynamic parameters for DNA reactions can account for the main forces contributing to DNA stability [37, 38]. If the enthalpy changes (ΔH^0) do not vary significantly over the temperature range studied, then its value could be determined from the Van't Hoff equation [39]:

$$\ln K = -\Delta H^0/RT + \Delta S^0/R \quad (4)$$

The free energy change ΔG^0 of the binding reaction at different temperature was estimated from the Eq. 5:

$$\Delta G^0 = \Delta H^0 - T\Delta S^0 \quad (5)$$

From the linear relationship between $\ln K$ and $1/T$, the value of ΔH^0 and ΔS^0 could be obtained. The ΔG^0 at different temperatures were calculated using Eq. 5, the results were presented in Table 3. Many references have reported the characteristic sign of the thermodynamic parameter associated with the various individual kinds of interaction that may take place in macromolecules association process [40, 41]. As shown in Table 3, the negative sign for ΔG^0 means that the binding process is spontaneous, $\Delta H^0 = -70.31 \text{ kJ mol}^{-1}$ means the formation of the DNR–D5–DNA complex is an exothermic reaction. Negative ΔH^0 and negative ΔS^0 indicate that hydrogen bonding forces most likely play a major role in the interaction of DNR–D5 with ctDNA [42]. Hydrogen bonding is a typical character for intercalating mode of drug with DNA [43, 44]. This result indicates again that the binding mode between DNR–D5 and ctDNA might be intercalation.

Molecular Modeling of DNR–D5 With ctDNA Interaction

Docking studies provide some insight into the interactions between the macromolecule and ligand, which can corroborate the experimental results [45]. The structure of ctDNA duplex 5'-d(CCATTAATGG)₂-3' was built and optimized by molecular mechanics in force field of CHARMM. The Discovery studio 2.1 program protocol was used for the docking of interactions between DNR–D5 and ctDNA. The docked model as shown in Fig. 6 suggests that the anthraquinone chromophore of DNR–D5

can slide into the C–G rich region of ctDNA. In addition, there are hydrogen interactions of C-2 amido hydrogen of G16 and the C-2 Carbonyl O atom of C9 with C-6 hydroxy O atoms, C-5 Carbonyl O atoms and C-6 hydroxy H atoms of DNR–D5. The length of the hydrogen bond is 2.12 Å, 1.67 Å, 1.61 Å and 2.35 Å, respectively. This indicates again that hydrogen bonding forces play an essential role in the binding of DNR–D5 to ctDNA. The results obtained from molecular docking corroborate the experimental results obtained from spectroscopic investigations. Thus it can be seen that there is a mutual complement between spectroscopy techniques and molecular modeling, which can provide fruitful information about the mechanism of interaction and the conformation of adduct from different aspects.

Conclusion

In this paper, the interaction of DNR–D5 with ctDNA was studied by UV/Vis in combination with fluorescence spectroscopy and molecular modeling techniques for the first time. We have investigated that fluorescence quenching mechanism of DNR–D5 by ctDNA is a static quenching type. The binding mode between DNR–D5 and ctDNA might be intercalation. Upon binding to ctDNA, the anthraquinone chromophore of DNR–D5 can slide into the C–G rich region of ctDNA. Hydrogen bonding forces play an essential role in the binding of DNR–D5 to ctDNA. Moreover, the large binding constant indicates that DNR–D5 have a high affinity with ctDNA. Thus DNR–D5 is expected to become one of the drug candidates. This work should be helpful for understanding the interaction of DNR–D5 with DNA and designing new anthracycline drugs.

Acknowledgements The authors are grateful to the National Natural Science Foundation of China (Grant no. 20673034 and 20672031), the Research Fund for the Doctoral Program of Higher Education of China (Grant no. 20060476001) and the program for Innovative Research Team in University of Henan Province (2008IRTSTHN002) for their financial supports.

References

1. Yang X, Wang AHJ (1999) Structural studies of atom-specific anticancer drugs acting on DNA. *Pharmacol Therapeut* 83:181–215
2. Chaires JB (2006) A thermodynamic signature for drug–DNA binding mode. *Arch Biochem Biophys* 453:26–31
3. Beraldo H, Garnier-Suillerot A, Tosi L, Lavelles F (1985) Iron(III)-adriamycin and Iron(III)-daunorubicin complexes: physicochemical characteristics, interaction with DNA, and antitumor activity. *Biochemistry* 24:284–289

4. Pang JY, Qin Y, Chen WH, Luo GA, Jiang ZH (2005) Synthesis and DNA-binding affinities of monomodified berberines. *Bioorgan Med Chem* 13:5835–5840
5. Singh MP, Joseph T, Kumar S, Bathini Y, Lown JW (1992) Synthesis and sequence-specific DNA binding of a topoisomerase inhibitory analog of Hoechst 33258 designed for altered base and sequence recognition. *Chem Res Toxicol* 5:597–607
6. Andrew WHJ, Giovanni U, Gary JQ, Alexander R (1987) Interactions between an anthracycline antibiotic and DNA: molecular structure of daunomycin complexed to d(CpGpTpApCpG) at 1.2 Å resolution. *Biochemistry* 26:1152–1163
7. Laurie LP, Fiona MA, Caroline O, Hare C, Stephen ML, John PB, David JR, John AH (2005) Synthesis of novel DNA cross-linking antitumour agents based on polyazamacrocycles. *Bioorgan Med Chem* 13:2389–2395
8. Rajender AK, Rajasekhar DR, Reddy MK, Balakishan G, Shaik TB, Chourasia M, Narahari Sastry G (2009) Remarkable enhancement in the DNA-binding ability of C2-fluoro substituted pyrrolo[2, 1-c][1, 4]benzodiazepines and their anticancer potential. *Bioorgan Med Chem* 17:1557–1572
9. Ivandini TA, Honda K, Rao TN, Fujishima A, Einaga Y (2007) Simultaneous detection of purine and pyrimidine at highly boron-doped diamond electrodes by using liquid chromatography. *Talanta* 71:648–665
10. Zunino F, Di Marco A, Zaccara A, Gambetta RA (1980) The interaction of daunorubicin and doxorubicin with DNA and chromatin. *Biochim Biophys Acta* 607:206–214
11. Li JF, Dong C (2009) Study on the interaction of morphine chloride with deoxyribonucleic acid by fluorescence method. *Spectrochim Acta Part A* 71:1938–1943
12. Takahara PM, Rosenzweig AC, Frederick CA, Lippard SJ (1995) Crystal structure of double-stranded DNA containing the major adduct of the anticancer drug cisplatin. *Nature* 377:649–652
13. Zhou BB, Elledge SJ (2000) The DNA damage response: putting checkpoints in perspective. *Nature* 408:433–439
14. Chifotides HT, Dunbar KR (2005) Interactions of Metal–Metal-Bonded Antitumor Active Complexes with DNA Fragments and DNA. *Acc Chem Res* 38:146–156
15. Waring M (1970) Validation of the supercoils in closed circular DNA by binding of antibiotics and drugs: evidence for molecular models involving intercalation. *J Mol Biol* 54:247–279
16. Chaires JB (2006) A thermodynamic signature for drug–DNA binding mode. *Arch Biochem Biophys* 453:26–31
17. Weiss RB, Sarosy G, Clagett-Carr K, Russo M (1986) Anthracycline analogs: the past, present, and future. *Cancer Chemoth Pharm* 18:185–197
18. Htun MT (2009) Photophysical study on Daunorubicin by fluorescence spectroscopy. *J Lumin* 129:344–348
19. Wang AHJ (1992) Intercalative drug binding to DNA. *Curr Opin Struct Biol* 2:361–368
20. Arcamone F (1981) In doxorubicin, anticancer antibiotics in medicinal chemistry series. Academic, New York
21. Zagotto G, Gatto B, Moro S, Sissi C, Palumbo M (2001) Anthracyclines: recent developments in their separation and quantitation. *J Chromatogr B* 764:161–171
22. Cui FL, Qin LX, Zhang GS, Liu QF, Yao XJ, Lei BL (2008) Interaction of anthracycline disaccharide with human serum albumin: investigation by fluorescence spectroscopic technique and modeling studies. *J Pharm Biomed Anal* 48:1029–1036
23. Fang LY, Zhang GS, Li CL, Zheng XC, Zhu LZ, Xiao JJ, Gergely S, Janos N, Chan KK, Wang PG, Sun DX (2006) Discovery of Daunorubicin analogue that exhibits potent antitumor activity and overcomes p-gp-mediated drug resistance. *J Med Chem* 49:932–941
24. Zhang GS, Fang LY, Zhu LZ, Aimiwu JE, Shen J, Muller MT, Lee GE, Sun DX, Wang PG (2005) Syntheses and biological activities of disaccharide daunorubicins. *J Med Chem* 48:5269–5278
25. Robert FB, Zhong YQ, Fang LY, Seth G, Jie S, Janos N, Zhang GS, Sun DX (2007) Modifying the sugar moieties of Daunorubicin overcomes p-gp-mediated multidrug resistance. *Mol Pharm* 4:140–153
26. Fukuda R, Takenaka S, Takagi M (1990) Metal ion assisted DNA-intercalation of crown ether-linked acridine derivatives. *J Chem Soc Chem Commun* 1028–1030
27. Kapuscinski J, Darzynkiewicz Z (1985) Interactions of antitumor agents Ametantrone and Mitoxantrone (Novatrone) with double-stranded DNA. *Biochem Pharmacol* 34:4203–4213
28. Dang XJ, Nie MY, Tong J, Li HL (1998) Inclusion of the parent molecules of some drugs with beta-cyclodextrin studied by electrochemical and spectrometric method. *J Electroanal Chem* 448:61–67
29. Li N, Ma Y, Yang C, Guo L, Yang XR (2005) Interaction of anticancer drug mitoxantrone with DNA analyzed by electrochemical and spectroscopic methods. *Biophys Chem* 116:199–205
30. Purcell M, Neault JF, Riahi T (2000) Interaction of taxol with human serum albumin. *Biochim Biophys Acta* 1478:61–68
31. Ibrahim MS (2001) Voltammetric studies of the interaction of nogalamycin antitumor drug with DNA. *Anal Chim Acta* 443:63–72
32. Bera R, Sahoo BK, Ghosh KS, Dasgupta S (2008) Studies on the interaction of isoxazolcurcumin with calf thymus DNA. *Int J Biol Macromol* 42:14–21
33. Ashoka S, Seetharamappa J, Kandagal PB, Shaikh SMT (2006) Investigation of the interaction between trazodone hydrochloride and bovine serum albumin. *J Lumin* 121:179–186
34. Lakowicz JR (1999) Principles of fluorescence spectroscopy. Plenum, New York
35. Lakowicz JR, Weber G (1973) Quenching of fluorescence by oxygen. Probe for structural fluctuations in macromolecules. *Biochemistry* 12:4161–4170
36. Ware WR (1962) Oxygen quenching of fluorescence in solution: an experimental study of the diffusion process. *J Phys Chem* 66:455–458
37. Yue YY, Zhang YH, Zhou L, Qin J, Chen XG (2008) In vitro study on the binding of herbicide glyphosate to human serum albumin by optical spectroscopy and molecular modeling. *J Photochem Photobiol B* 90:26–32
38. Cui FL, Qin LX, Zhang GS, Yao XJ, Du J (2008) Binding of daunorubicin to human serum albumin using molecular modeling and its analytical application. *Int J Biol Macromol* 42:221–228
39. Bi SY, Song DQ, Tian Y, Zhou X, Liu ZY, Zhang HQ (2005) Molecular spectroscopic study on the interaction of tetracyclines with serum albumins. *Spectrochim Acta Part A* 61:629–636
40. Juziro N, Noriko M (1985) Binding parameters of theophylline and aminophylline to bovine serum albumin. *Chem Pharm Bull* 33:2522–2524
41. Neméthy G, Scheraga HA (1962) Structure of water and hydrophobic in proteins. *J Phys Chem* 66:1773–1789
42. Ross PD, Subramanian S (1981) Thermodynamics of protein association reactions: forces contributing to stability. *Biochemistry* 20:3096–3102
43. Takenaka S, Ihara T, Takagi M (1990) Bis-9-acridinyl derivative containing a viologen linker chain: electrochemically active intercalator for reversible labelling of DNA. *J Chem Soc Chem Commun* 1485–1487
44. Xu Y, Jing Y, Cai H, Fang YZ (2004) Electrochemical impedance detection of DNA hybridization based on the formation of M-DNA on polypyrrole/carbon nanotube modified electrode. *Anal Chim Acta* 516:19–27
45. Tan J, Wang BC, Zhu LC (2009) DNA binding cytotoxicity apoptotic inducing activity, and molecular modeling study of quercetin zinc(II) complex. *Bioorgan Med Chem* 17:614–620